Optimal coordination of flexible resources in the gas-heat-electricity integrated energy system

Xi, Yufei; Fang, Jiakun; Chen, Zhe; Zeng, Qing; Lund, Henrik

Published in:
Energy

DOI (link to publication from Publisher):
10.1016/j.energy.2020.119729

Publication date:
2021

Document Version
Accepted author manuscript, peer reviewed version

Optimal Coordination of Flexible Resources in the Gas-heat-electricity Integrated Energy System

Yufei Xi [a], Jiakun Fang [b], Zhe Chen [a] *, Qing Zeng [c], Henrik Lund [d]

[a] *Department of Energy Technology, Aalborg University, 9220, Aalborg, Denmark*

[b] *State Key Lab of Advanced Electromagnetic Engineering and Technology, School of Electrical and Electronic Engineering, Huazhong University of Science and Technology, Wuhan 430074, China*

[c] *Sichuan Energy Internet Research Institute, Tsinghua University, 610000, Chengdu, Sichuan, China*

[d] *Department of Development and Planning, Aalborg University, 9000 Aalborg, Denmark*

***Abstract*:** To deal with the high penetration of renewable energy, modern energy systems strive to introduce flexible resources to provide more flexible and higher quality services. This paper focuses on the coordination of flexible resources across different energy carriers under the market environment to accommodate different levels of wind power. The integration of gas, heat and electricity systems providing customers with multiple options for satisfying their energy demands is described. Considering that energy system operators are independent or have limited communication based on the existing market mechanism, an equilibrium problem is first formulated for the optimal scheduling strategy, where each subsystem operator pursues its own benefit. Since there is energy conversion between different energy subsystems, each subsystem operator has to consider the actions of other operators and coordinate with each other until an equilibrium. An illustrative case study is then analyzed to show that the proposed model allows each subsystem operator to make an optimal action for maximizing its profit, and reflects prices and volumes of the energy transaction among energy subsystems. Furthermore, the simulation results indicate that the coordination of flexible resources has significant benefits in the integrated energy system to reduce wind curtailment and improve total social welfare.

***Index Terms*:** Flexible resource; integrated energy system; coordination; demand response; energy market; equilibrium problem.

NOMENCLATURE

Parameters	Description [Unit]
P_t^{l}	Power load of the EPS at time t [MW]
G_t^{l}	Gas load of the NGS at time t [MW]
H_t^{l}	Heat load of the DHS at time t [MW]
Variables	
p_t^{e}	Electricity price at time t [€/MWh]
p_t^{g}	Gas price at time t [€/MWh]
$P_{i,t}^{\mathrm{CFP}}$	Power generation of CFP unit i at time t [MW]
$P_{i,t}^{\mathrm{CHP}}$	Power generation of CHP unit i at time t [MW]
$P_{i,t}^{\mathrm{EB}}$	Power consumption of EB unit i at time t [MW]
$P_{i,t}^{\mathrm{P2G}}$	Power consumption of P2G unit i at time t [MW]
$P_{i,t}^{\mathrm{shift}}$	Power load shifted from bus i at time t [MW]
$P_{i,t}^{\mathrm{W}}$	Power generation of wind turbine i at time t [MW]
$\delta_{m,t}$	Phase angle of bus m at time t [rad]
$G_{j,t}^{\mathrm{SN}}$	Gas generation of gas source j at time t [MW]
$G_{j,t}^{\mathrm{CHP}}$	Gas consumption of CHP unit j at time t [MW]
$G_{j,t}^{\mathrm{GB}}$	Gas consumption of GB j at time t [MW]
$G_{j,t}^{\mathrm{P2G}}$	Gas generation of P2G unit j at time t [MW]
$G_{j,t}^{\mathrm{c}}/G_{j,t}^{\mathrm{d}}$	Charged/discharged gas power of gas storage j at time t [MW]
$SOC_{j,t}^{\mathrm{GS}}$	SOC of gas storage j at time t [MWh]
$G_{mn,t}$	Gas power through pipeline m-n at time t [MW]

$p_{m,t}$	Gas pressure of node *m* at time *t* [MPa]
$G^{in}_{mn,t}/G^{ex}_{mn,t}$	The injection and extraction of the gas flows in pipeline *m*-*n* at time *t* [MW]
$LP_{mn,t}$	The amount of linepack storage in pipeline *m*-*n* at time *t* [MWh]
$H^{CHP}_{k,t}$	Heat generation of CHP unit *k* at time *t* [MW]
$H^{GB}_{k,t}$	Heat generation of GB *k* at time *t* [MW]
$H^{EB}_{k,t}$	Heat generation of EB *k* at time *t* [MW]
$H^{c}_{k,t}/H^{d}_{k,t}$	Charged/discharged heat power of heat storage *k* at time *t* [MW]
$SOC^{HS}_{k,t}$	SOC of heat storage *k* at time *t* [MWh]
$H_{mn,t}$	Heat power through pipeline *m*-*n* at time *t* [MW]
$T_{m,t}$	Temperature of water flow at node *m* at time *t* [℃]

Acronyms

IES	Integrated Energy System
GHE-IES	Gas-heat-electricity Integrated Energy System
EPS	Electric Power System
NGS	Natural Gas System
DHS	District Heating System
FR	Flexible Resource
CHP	Combined Heat and Power
P2G	Power to Gas
EB	Electric boiler
CFP	Coal-fired power
DR	Demand Response
LPF	Load Participation Factor

SOC	State of Charge
GN/HN	Gas Node/Heat Node

1. Introduction

With growing policy incentives and public awareness on climate change and risks, the global energy structure is experiencing a vital transition to sustainable energy sources [1]. Many countries around the world have set ambitious targets replacing fossil fuel. For instance, the Danish Commission on Climate Change Policy reported that Denmark could be independent of fossil fuel for all energy sectors by 2050 [2]. In order to achieve these targets and accommodate the growing renewable energy, fully using energy conversion technologies such as combined heat and power (CHP), the power to gas (P2G), electric boilers (EBs), etc., the integrated energy system (IES) has received great attention and developed rapidly in recent years [3-5].

However, the complementation and integration of multiple energy sectors cause higher requirements for the flexibility of IESs [6]. Facing this challenge, adopting flexible resources (FRs) is a critical and effective measure to improve the flexibility of IESs. FRs can refer to some energy equipment such as quick-dispatched units, energy storage devices, etc., as well as some control methods such as demand response (DR) management. In fact, they are introduced to ensure flexible energy supply, transmission, demand and system operations, and help maintain the balance between supply and demand of different energy systems [7].

In literatures, different FRs have been respectively used to participate in the operation of the corresponding energy system. For the electric power system (EPS), the common FRs include DR, batteries/bulk energy storage, plug-in electric vehicles, etc. Reference [8] considers DR, storage systems and plug-in electric vehicle parking lots, and develops an integrated stochastic day-ahead market-clearing model to achieve flexible scheduling of the EPS. For the natural gas system (NGS), the common FRs include gas linepack, gas tanks, etc. Besides, with gas-fired plants and P2G technologies, the NGS and EPS may provide flexibility to each other when interlinking. Reference [9] considers gas linepack and energy storage, and formulates a scheduling model for the optimal operation of the gas-electricity IES. Reference [10] adopts DR

management through P2G in an expansion model for the gas-electricity IES, and shows that this kind of DR can relieve grid congestion and reduce electricity prices. For the district heating system (DHS), besides flexible heat storage devices, references [11] and [12] indicate that the thermal inertia of buildings and the storage capacity of heating pipelines are also applicable FRs.

Obviously, the integration and coordination of FRs across different energy systems are important issues. The integration of IESs and corresponding optimization algorithms have been widely discussed and studied. Reference [13] establishes a dual objective operation optimization model of IES and proposes an integrated demand response mechanism. Reference [14] proposes a multi-stage contingency-constrained co-planning model for electricity-gas systems considering the uncertainties of load demand and wind power. To solve the problem, an iterative Benders decomposition method is developed to divide the programming into one master investment problem and three subproblems. Reference [15] proposes a hybrid approach combining heuristic and analytical optimization for the gas-electricity IES in western Denmark. The simulation result indicates the beneficial role of the FRs to improve wind power accommodation.

However, to date, most of the existing research is based on the assumption that there is a central operator that controls the multiple resources, integrates and operates all energy systems in pursuit of a certain overall objective. However, in the actual market environment, each energy system operator may pursue its own benefit with limited communication (due to the confidentiality of company data). Game theory provides a solution to analyze such interactions and competitions between the system operators. In [16], a game approach for demand-side consumption is applied to optimize the system scheduling and to reduce the information collection. In [17], considering distributed generations and batteries, a market model is proposed for the dispatch of virtual power plants. In [18], a modeling approach is developed for the gas and electricity markets. The proposed multiple-leader/two-follower complementarity problem can find equilibria with different objectives, e.g., maximized social welfare, producer profits, or consumer benefits.

Inspired by the applications of game theory in the market environment, this paper investigates the optimal coordination of FRs in the gas-heat-electricity integrated energy system (GHE-IES), covering

intelligent supply operations, flexible energy demand and multiple energy storages. To better observe the energy distribution and market performance of the GHE-IES in the coordinated operation, it is assumed that each subsystem operator acts as an independent player to pursue its own benefit maximization until an equilibrium. An equilibrium problem is proposed to model the behaviors of energy subsystem operators in the market. After linearization, the optimization problem of the proposed model can be replaced by jointly solving Karush-Kuhn-Tucker (KKT) conditions [19].

The major contributions and highlights of this paper are: (1) the integration of gas, heat and electricity systems providing customers with multiple options of energy supply is described; (2) an equilibrium model for coordinating flexible resources to optimally dispatch the energy generation and perform energy trading is proposed; (3) the proposed model is simulated in two scenarios of high-wind power and low-wind power, and the effect of wind power levels on market behaviors and system operations is discussed; (4) different demand response participation levels are introduced to further explore the positive impacts of demand response management.

The remainder of the paper is organized as follows. Section 2 describes the structure of the GHE-IES and introduces the utilization of FRs. Section 3 formulates the optimization problem and presents the solution methodology. Section 4 illustrates the simulation results and discusses a case study. Section 5 draws the conclusions.

2. Gas-heat-electricity integrated energy system

In this section, the proposed GHE-IES is a combination of an EPS, a DHS and a NGS, which supplies gas, heat and electricity for consumers, respectively. The structure of the GHE-IES is based on a typical urban energy supply system in Denmark. For simplicity, wind is considered the only source of renewable energy for the IES, and the fuel of each CHP unit is natural gas.

2.1 Description of the gas-heat-electricity integrated energy system

The schematic graph of the GHE-IES with FRs is shown in Fig. 1. Each subsystem (EPS, NGS or DHS)

has an independent operator to maintain its energy balance between supply and demand, and control its energy trading with other subsystems.

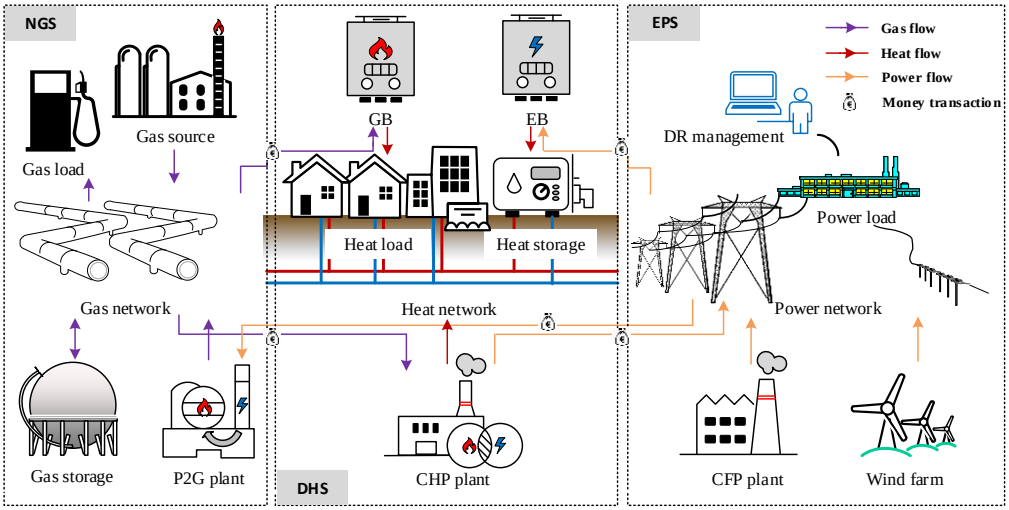

Fig. 1. Schematic graph of the GHE-IES with FRs.

Fig. 1 shows the energy generation, conversion and consumption of each energy subsystem. The NGS involves gas sources, P2G plants, gas storages, gas loads and the gas network. As an energy converter that consumes electricity to produce gas, the P2G plant is controlled by the NGS operator to assist the gas supply and to accommodate the surplus wind power. The EPS includes coal-fired power (CFP) plants, wind farms, power loads with DR management and the power network. The DHS consists of CHP plants, EBs, gas boilers (GBs), heat storages, heat loads and the heat network. EBs and GBs controlled by the DHS operator supply heat by consuming electricity and gas, respectively. Generally, EBs have a faster startup than heat pumps. For some big cities in Denmark, such as Copenhagen, the DHS also uses heat pumps to supply heat. Although modern EBs have a much-improved efficiency (around 90%), this efficiency is still much lower than that of heat pumps. The efficiency of heat pumps can reach as high as 350% leading to its great potential in future energy markets [20]. CHP plants controlled by the DHS operator consume gas to supply heat. Since the heat and electricity production are coupled, each CHP unit has to operate within a feasible boundary [21].

The subsystem operators may participate in the energy exchange of the market as a prosumer, i.e. both energy buyer/consumer and seller/producer. For example, the NGS is a prosumer. On the one hand, it sells gas to the DHS to run CHP units and GBs. On the other hand, it may buy electricity from the EPS to run P2G units when there is a surplus of wind power leading to a low electricity price. The EPS also acts as a prosumer. It may buy electricity from CHP plants, and sell electricity to the DHS to run EBs or to the NGS to run P2Gs. It should be noted that the DHS acts as a pure consumer. In order to meet its heat demand, it needs to purchase gas from the NGS as well as electricity from the EPS. In other words, the heat demand can be considered as a welfare product for the EPS and the DHS to satisfy their own demand, which is consistent with the actual situation of the non-profit heat market in Denmark [22].

2.2 Utilization and modeling of flexible resources

In the GHE-IES, the integration of energy networks enables conversion between different energy carriers in which different FRs can coordinate with each other. In this paper, the applicable FRs include the flexible integrated energy demand achieved by multiple energy conversion, DR management achieved by the communication and the control system of the EPS, and multiple energy storages.

2.2.1 Flexible supply options by energy conversion

Energy conversion facilities enable the energy generation no longer limited to a single energy system. For instance, the option of gas supply through P2G units is not only a way to integrate the EPS, but also a way to adjust the electricity demand. Since NGSs and EPSs are generally for bulk energy transmission across a country or a continent, most research of them mainly pertains to a transmission level. In comparison, the DHS is focused on a local level of an urban or a district because of the higher cost and heat energy loss for long-distance transmission. Hence, from the perspective of the NGS and the EPS, the DHS can be considered as a pure consumer of integrated electricity and gas. The multiple heating options achieved by EBs, GBs and CHP units indirectly offer an opportunity to adjust the electricity and gas demands. In the tth time period, the electricity demand (P_t^{D}) and the gas demand (G_t^{D}) can be expressed as:

$$P_t^{\mathrm{D}} = P_t^{\mathrm{l}} + \sum_{i=1}^{I^{\mathrm{EB}}}\left(P_{i,t}^{\mathrm{EB}}\right) + \sum_{i=1}^{I^{\mathrm{P2G}}}\left(P_{i,t}^{\mathrm{P2G}}\right) \quad \forall t \in T \tag{1}$$

$$G_t^{\mathrm{D}} = G_t^{\mathrm{l}} + \sum_{j=1}^{J^{\mathrm{CHP}}}\left(G_{j,t}^{\mathrm{CHP}}\right) + \sum_{j=1}^{J^{\mathrm{GB}}}\left(G_{j,t}^{\mathrm{GB}}\right) \quad \forall t \in T \tag{2}$$

where T is the set of time periods. I^{EB} and I^{P2G} identify the set of buses connecting EBs and P2G unit, respectively. J^{CHP} and J^{GB} identify the set of nodes connecting CHP units and GBs, respectively. Eq. (1) defines the power demand of the EPS at time t including three components: the power load of all consumers, the power consumption for the DHS to run EBs and the power consumption for the NGS to run P2G units. Eq. (2) defines the gas demand of the NGS at time t including three components: the gas load of all consumers, the gas consumption for the DHS to run CHP units and GBs. Meanwhile, at time t, the multiple heat suppliers controlled by the DHS to meet the heat demand (H_t^{D}):

$$H_t^{\mathrm{D}} = \sum_{k=1}^{K^{\mathrm{CHP}}}\left(H_{k,t}^{\mathrm{CHP}}\right) + \sum_{k=1}^{K^{\mathrm{GB}}}\left(H_{k,t}^{\mathrm{GB}}\right) + \sum_{k=1}^{K^{\mathrm{EB}}}\left(H_{k,t}^{\mathrm{EB}}\right) \quad \forall t \in T \tag{3}$$

where K^{CHP}, K^{GB} and K^{EB} are the set of nodes connecting CHP units, GBs and EBs, respectively. Eq. (3) defines the heat demand of the DHS at time t that is equal to the sum of the heat generation of CHPs, GBs and EBs.

2.2.2 DR management

As a typical FR on the demand side, the EPS operator also adopts DR management to encourage its consumers to change the consumption pattern in a beneficial way. DR management was originally proposed by Schweppe's et al. in 1988 [23]. They design a system where consumers can adjust their loads based on the spot price of electricity, while the electricity price will be updated in real time based on the adjusted loads. In the follow-up research, DR is divided into time-based program and incentive-based program [24]. Based on the real-time DR model developed in [25] and hourly DR model proposed in [26], the tth power load of the EPS is divided into the base load (P_t^{bl}) and the response load (P_t^{rl}).

$$P_t^{\mathrm{l}} = P_t^{\mathrm{bl}} + P_t^{\mathrm{rl}} \quad \forall t \in T \tag{4}$$

The base load is the power consumption for consumers to satisfy their basic requirements, and it corresponds to a compulsory energy need. The response load controlled by the DR management participates in the market and responds to the spot price. To represent the relationship between the base load and the response load, Eq. (5) introduces and defines the load participation factor (LPF) as follows.

$$\mathrm{LPF} = P_t^{\mathrm{rl}} \Big/ P_t^{\mathrm{l}} = P_t^{\mathrm{rl}} \Big/ \left(P_t^{\mathrm{rl}} + P_t^{\mathrm{bl}} \right) \quad \forall t \in T, \mathrm{LPF} \in (0,1) \tag{5}$$

Therefore, the mathematical model of DR management can be expressed as:

$$P_t^{\mathrm{lDR}} = P_t^{\mathrm{l}} - \sum_{i=1}^{I^{\mathrm{PL}}} P_{i,t}^{\mathrm{shift}} \qquad \forall t \in T \tag{6}$$

$$\left| \sum_{i=1}^{I^{\mathrm{PL}}} P_{i,t}^{\mathrm{shift}} \right| \le \mathrm{LPF} \cdot P_t^{\mathrm{l}} \qquad \forall t \in T \tag{7}$$

$$\sum_{t=1}^{T} \left(\sum_{i=1}^{I^{\mathrm{PL}}} P_{i,t}^{\mathrm{shift}} \right) = 0 \tag{8}$$

where I^{PL} identifies the set of load buses of the EPS. Eq. (6) defines the hourly-improved load (P_t^{lDR}) after DR management. $P_{i,t}^{\mathrm{shift}}$ is positive when the load is shifted out from bus i at time t, and negative when the load is shifted to bus i at time t. $\sum_{i=1}^{I^{\mathrm{PL}}} P_{i,t}^{\mathrm{shift}}$ represents the power load shifting of the EPS at time t, which is the sum of power load shifting of all load buses. Constraints (7) and (8) describe limits of load shifting at time t and restoration of load shifting within the scheduling period T, respectively. Additionally, in order to ensure that the increased/decreased load per unit time is within a reasonable range, the constraint of the rate of the original load change is expressed as:

$$\left| P_t^{\mathrm{lDR}} - P_{t-1}^{\mathrm{lDR}} \right| \le \left| P_t^{\mathrm{l}} - P_{t-1}^{\mathrm{l}} \right| \qquad \forall t \in T \tag{9}$$

Since the DR management can adjust the hourly power load of the EPS by shifting the proper load from/to another time period, the hourly electricity demand of the EPS given in Eq. (1) can be further expressed as:

$$\begin{aligned} P_t^{\mathrm{D}} &= P_t^{\mathrm{l}} - \sum_{i=1}^{I^{\mathrm{PL}}} P_{i,t}^{\mathrm{shift}} + \sum_{i=1}^{I^{\mathrm{EB}}} \left(P_{i,t}^{\mathrm{EB}}\right) + \sum_{i=1}^{I^{\mathrm{P2G}}} \left(P_{i,t}^{\mathrm{P2G}}\right) \\ &= P_t^{\mathrm{lDR}} + \sum_{i=1}^{I^{\mathrm{EB}}} \left(P_{i,t}^{\mathrm{EB}}\right) + \sum_{i=1}^{I^{\mathrm{P2G}}} \left(P_{i,t}^{\mathrm{P2G}}\right) \quad \forall t \in T \end{aligned} \tag{10}$$

2.2.3 Energy storages

In this GHE-IES, heat storages and gas storages are used to offer more flexibility to the corresponding energy subsystems. Based on the model formulated by references [27] and [28], Eq. (11) and Eq. (12) define the mathematical models of gas storage and heat storage, respectively. Each of them includes four components: limits of charging/discharging, energy balance in the storage device, limits of the storage capacity and storage restoration. The formulas are as follow:

$$\begin{cases} 0 \le G_{j,t}^{\mathrm{c}} \le G_j^{\mathrm{c,max}}, 0 \le G_{j,t}^{\mathrm{d}} \le G_j^{\mathrm{d,max}} \\ SOC_{j,t}^{\mathrm{GS}} - SOC_{j,t-1}^{\mathrm{GS}} = \left(G_{j,t}^{\mathrm{c}} - G_{j,t}^{\mathrm{d}}\right)\Delta t \\ 0 \le SOC_{j,t}^{\mathrm{GS}} \le SOC_j^{\mathrm{GS,max}} \\ SOC_{i,t_0}^{\mathrm{GS}} = SOC_{i,t_{\mathrm{N}}}^{\mathrm{GS}} \end{cases}, \forall j \in J^{\mathrm{GS}}, \forall t \in T \tag{11}$$

$$\begin{cases} 0 \le H_{k,t}^{\mathrm{c}} \le H_k^{\mathrm{c,max}}, 0 \le H_{k,t}^{\mathrm{d}} \le H_k^{\mathrm{d,max}} \\ SOC_{k,t}^{\mathrm{HS}} - \sigma SOC_{k,t-1}^{\mathrm{HS}} = \left(H_{k,t}^{\mathrm{c}} \eta_k^{\mathrm{c}} - H_{k,t}^{\mathrm{d}} / \eta_k^{\mathrm{d}}\right)\Delta t \\ 0 \le SOC_{k,t}^{\mathrm{HS}} \le SOC_k^{\mathrm{HS,max}} \\ SOC_{k,t_0}^{\mathrm{HS}} = SOC_{k,t_{\mathrm{N}}}^{\mathrm{HS}} \end{cases}, \forall k \in K^{\mathrm{HS}}, \forall t \in T \tag{12}$$

where J^{GS} and K^{HS} identify the set of nodes connected to gas storages in the NGS and heat storages in the DHS, respectively. $G_j^{\mathrm{c,max}}/G_j^{\mathrm{d,max}}$ is the maximum charge/discharge power of the gas storage j. $H_k^{\mathrm{c,max}}/H_k^{\mathrm{d,max}}$ is the maximum charge/discharge power of the heat storage k. Different from the gas storage, the heat loss occurs during the period of heat storage. Thus, there are three parameters to reflect the heat loss including self-discharged rate (σ), charged efficiency (η_k^{c}) and discharged efficiency (η_k^{d}). $SOC_j^{\mathrm{GS,max}}$ and $SOC_k^{\mathrm{HS,max}}$ are the maximum state of charge (SOC) of the gas storage j and the heat storage k, respectively. t_0 and t_{N} are the initial and end time of the storage during the scheduling period T.

3. Equilibrium formulation and solution methodology

As discussed in Section 1, most centralized optimizations of the IES assume that there is a central system operator to make an optimal strategy, where all subsystem operators have to cooperate to achieve a unified objective. However, in fact, different subsystems may have their own internal information protection mechanisms resulting in limited coordination between them. Under the limited communication, each subsystem operator is willing to pursue its own benefit rather than an overall profit. In this section, each energy subsystem (EPS, NGS and DHS) of the GHE-IES is assumed to be an independent operator to maximize its profit, which can be formulated as a Nash equilibrium problem [29].

3.1 Optimization objectives and decision variables

The equilibrium problem is composed of the optimization problems of the three subsystems (NGS EPS and DHS). The energy conversion and market actions of three subsystem operators are shown in Fig. 2.

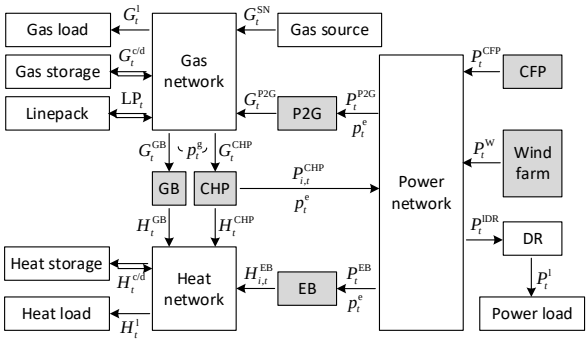

Fig. 2. The Nash equilibrium of the GHE-IES market modeling.

For simplicity, the fuel cost of the generation units is regarded as the operational cost of the system [30]. Each operator aims at maximizing its social welfare of the subsystem considering its own operational constraints. In each optimal operation model, the objective is defined as the producers' surplus plus the consumers' surplus. In this paper, the objective functions are expressed as negative profits. Thus, they are minimized as:

$$\min_{\boldsymbol{x}^{\mathrm{EPS}}} \sum_{t=1}^{T} \left\{ \sum_{i=1}^{I^{\mathrm{CFP}}} c_i^{\mathrm{CFP}} P_{i,t}^{\mathrm{CFP}} + \sum_{i=1}^{I^{\mathrm{CHP}}} p_t^{\mathrm{e}} P_{i,t}^{\mathrm{CHP}} - \sum_{i=1}^{I^{\mathrm{EB}}} p_t^{\mathrm{e}} P_{i,t}^{\mathrm{EB}} - \sum_{i=1}^{I^{\mathrm{P2G}}} p_t^{\mathrm{e}} P_{i,t}^{\mathrm{P2G}} - u^{\mathrm{PL}} P_t^{\mathrm{IDR}} \right\} \tag{13}$$
$$\boldsymbol{x}^{\mathrm{EPS}} = \left[P_{i,t}^{\mathrm{CFP}}, P_{i,t}^{\mathrm{W}}, P_{i,t}^{\mathrm{shift}} \right]$$

$$\min_{\boldsymbol{x}^{\mathrm{NGS}}} \sum_{t=1}^{T} \left\{ \sum_{j=1}^{J^{\mathrm{SN}}} c_j^{\mathrm{SN}} G_{j,t}^{\mathrm{SN}} + \sum_{i=1}^{I^{\mathrm{P2G}}} p_t^{\mathrm{e}} P_{i,t}^{\mathrm{P2G}} + \sum_{j=1}^{J^{\mathrm{GS}}} \left(c_j^{\mathrm{c}} G_{j,t}^{\mathrm{c}} + c_j^{\mathrm{d}} G_{j,t}^{\mathrm{d}} \right) - \sum_{j=1}^{J^{\mathrm{CHP}}} p_t^{\mathrm{g}} G_{j,t}^{\mathrm{CHP}} - \sum_{j=1}^{J^{\mathrm{GB}}} p_t^{\mathrm{g}} G_{j,t}^{\mathrm{GB}} - u^{\mathrm{GL}} G_t^{\mathrm{l}} \right\} \tag{14}$$
$$\boldsymbol{x}^{\mathrm{NGS}} = \left[G_{j,t}^{\mathrm{SN}}, G_{j,t}^{\mathrm{c}}, G_{j,t}^{\mathrm{d}}, G_{j,t}^{\mathrm{P2G}} \right]$$

$$\min_{\boldsymbol{x}^{\mathrm{DHS}}} \sum_{t=1}^{T} \left\{ \sum_{j=1}^{J^{\mathrm{CHP}}} p_t^{\mathrm{g}} G_{j,t}^{\mathrm{CHP}} + \sum_{j=1}^{J^{\mathrm{GB}}} p_t^{\mathrm{g}} G_{j,t}^{\mathrm{GB}} + \sum_{i=1}^{I^{\mathrm{EB}}} p_t^{\mathrm{e}} P_{i,t}^{\mathrm{EB}} + \sum_{k=1}^{K^{\mathrm{HS}}} \left(c_k^{\mathrm{c}} H_{k,t}^{\mathrm{c}} + c_k^{\mathrm{d}} H_{k,t}^{\mathrm{d}} \right) - \sum_{i=1}^{I^{\mathrm{CHP}}} p_t^{\mathrm{e}} P_{i,t}^{\mathrm{CHP}} - u^{\mathrm{HL}} H_t^{\mathrm{l}} \right\} \tag{15}$$
$$\boldsymbol{x}^{\mathrm{DHS}} = \left[H_{k,t}^{\mathrm{CHP}}, H_{k,t}^{\mathrm{c}}, H_{k,t}^{\mathrm{d}}, H_{k,t}^{\mathrm{GB}}, H_{k,t}^{\mathrm{EB}} \right]$$

where I^{CFP} and I^{CHP} identify the set of buses connecting CFP units and CHP units in the EPS, respectively. J^{SN} identifies the set of gas source nodes. u^{PL}, u^{GL} and u^{HL} represent the marginal utility of consumers' electricity consumption, gas consumption and heat consumption, respectively. c_i^{CFP} is the marginal cost of power production from CFP unit *i*. c_j^{SN} is the marginal cost of gas production from gas source *j*. $c_j^{\mathrm{c}}/c_j^{\mathrm{d}}$ and $c_k^{\mathrm{c}}/c_k^{\mathrm{d}}$ represent the charged/discharged marginal cost of gas storage *j* and heat storage *k*, respectively.

Eq. (13) represents the objective of the EPS and includes five components: the operational cost of CFP units, the cost of buying electricity from CHP plants, the revenue from selling electricity to the DHS for running EBs, the revenue from selling electricity to the NGS for running P2G units, and the total utility for actual electricity consumption of consumers after DR improvement. Eq. (14) represents the objective of the NGS and includes six components: the operational cost of gas supply from gas sources, the cost of buying electricity for P2G plants, the operational cost of charged/discharged gas of gas storages, the revenue from selling gas to the DHS for running CHP plants and GBs, and the total utility for gas consumption of consumers. Eq. (15) represents the objective of the DHS and includes six components: the cost of buying gas from the NGS to run CHP plants and GBs, the cost of buying electricity from the EPS to run EBs, the operational cost of charged/discharged heat of heat storages, the revenue from selling electricity to the EPS for power supply, and the total utility for heat consumption of consumers.

In this equilibrium problem, the decision variables $P_{i,t}^{\mathrm{CHP}}$, $P_{i,t}^{\mathrm{EB}}$, $P_{i,t}^{\mathrm{P2G}}$, $G_{j,t}^{\mathrm{CHP}}$, and $G_{j,t}^{\mathrm{GB}}$ linking the energy subsystems reflect the energy exchange between them. The energy exchange takes places in the energy market in which each subsystem operator pays or charges with other operators. The decision variables of energy prices p_t^{e} and p_t^{g} represent the trading prices of the market. It should be noted that the action of any subsystem operator will influence the actions of the other operators. For the EPS, the decision variables are $P_{i,t}^{\mathrm{CFP}}$, $P_{i,t}^{\mathrm{shift}}$ and $P_{i,t}^{\mathrm{W}}$. For the NGS, the decision variables are $G_{j,\mathrm{t}}^{\mathrm{SN}}$, $G_{j,t}^{\mathrm{c/d}}$ and $G_{j,t}^{\mathrm{P2G}}$. For the DHS, the decision variable are $H_{k,\mathrm{t}}^{\mathrm{CHP}}$, $H_{k,t}^{\mathrm{c/d}}$, $H_{k,t}^{\mathrm{GB}}$ and $H_{k,t}^{\mathrm{EB}}$. In each subsystem, the market clearing conditions enforce the energy balance between supply and demand.

3.2 Optimization constrains

The decision variables of each subsystem are subject to its operational constraints. The decision variables of the gas and electricity prices obtained by solving the equilibrium problem depend on the decision variables of all subsystems.

3.2.1 EPS constrains

In the EPS, the real power should be balanced for each time period.

$$\sum_{i=1}^{I^{\mathrm{CHP}}} P_{i,t}^{\mathrm{CHP}} + \sum_{i=1}^{I^{\mathrm{CFP}}} P_{i,t}^{\mathrm{CFP}} + \sum_{i=1}^{I^{\mathrm{WF}}} P_{i,t}^{\mathrm{W}} - P_t^{\mathrm{D}} = \sum_{m=1}^{\Lambda^{\mathrm{n}}} B_{mn}\left(\delta_{m,t} - \delta_{n,t}\right) \qquad \forall n \in I, \forall t \in T \tag{16}$$

where I sets the buses of the EPS. I^{WF} identifies the set of buses connecting wind farms. Λ^{n} identifies the set of buses directly connecting to bus n. B_{mn} represents line susceptance from bus m to n. The power network constraint uses the DC power flow, which can be obtained from the nodal phase angles through the transmission line m-n. Thus, the limits of the transmission capacity can be expressed as:

$$\left|B_{mn}\left(\delta_{m,t} - \delta_{n,t}\right)\right| \le P_{mn}^{\max} \qquad \forall m, n \in I, \forall t \in T \tag{17}$$

where $P_{mn}^{\max}$ is the maximum power allowed by the transmission line m-n. The power output limits of the generators are expressed as:

$$P_i^{\min} \le P_{i,t} \le P_i^{\max} \quad \forall i \in I^{\mathrm{CHP}} \cup I^{\mathrm{CFP}} \cup I^{\mathrm{WF}}, \forall t \in T \tag{18}$$

where $P_i^{\min}$/ $P_i^{\max}$ is the minimum/maximum operation power of the generator i in the EPS. The ramping limits excluding the wind farms are expressed as:

$$\left|P_{i,t} - P_{i,t-1}\right| \le P_i^{\mathrm{R}} \quad \forall i \in I^{\mathrm{CHP}} \cup I^{\mathrm{CFP}}, \forall t \in T \tag{19}$$

where P_i^{R} is the ramping limit for the generator i.

3.2.2 NGS constrains

In the NGS, the transportation of gas is subject to the nodal gas balance, which is expressed as [15]:

$$\sum_{j=1}^{J^{\mathrm{SN}}} G_{j,t}^{\mathrm{SN}} + \sum_{j=1}^{J^{\mathrm{P2G}}} G_{j,t}^{\mathrm{P2G}} + \sum_{j=1}^{J^{\mathrm{GS}}} \left(G_{j,t}^{\mathrm{d}} - G_{j,t}^{\mathrm{c}}\right) + \sum_{m=1}^{\Lambda^{\mathrm{n}}} \left(G_{mn,t}^{\mathrm{ex}} - G_{mn,t}^{\mathrm{in}}\right) - G_t^{\mathrm{D}} = \sum_{m=1}^{\Lambda^{\mathrm{n}}} G_{mn,t} \quad \forall n \in J, \forall t \in T \tag{20}$$

where J sets the nodes of the NGS. J^{P2G} identifies the set of nodes connecting P2G units. The gas network follows the principle that gas flows from nodes with higher pressure to lower pressure [9]. In the isothermal gas pipeline *m*-*n*, the relationship between gas power flow and nodal gas pressure is determined as:

$$Z_{mn}\left(G_{mn,t}\right)^2 = p_{m,t}^2 - p_{n,t}^2 \quad \forall m, n \in J, \forall t \in T \tag{21}$$

where Z_{mn} represents the resistance coefficient of the pipeline *m*-*n*. The limits of the gas transmission capacity can be expressed as:

$$\left|G_{mn,t}\right| \le G_{mn}^{\max} \quad \forall m, n \in J, \forall t \in T \tag{22}$$

where $G_{mn}^{\max}$ is the maximum gas power flow allowed by the gas pipeline *m*-*n*. The gas output limits of the producers in the NGS are expressed as:

$$G_j^{\min} \le G_{j,t} \le G_j^{\max} \quad \forall j \in J^{\mathrm{SN}} \cup J^{\mathrm{P2G}}, \forall t \in T \tag{23}$$

where $G_j^{\min}$/ $G_j^{\max}$ is the minimum/maximum gas output of the gas producer j.

In dynamic situations of the NGS, linepack, the total amount of gas present in gas pipelines, plays a role in balancing the gas production and consumption [29]. Linepack can be determined by the accumulated difference between the injection and extraction of the gas flows in the pipeline [9]. Eq. (24) gives the

constraints of gas linepack *m*-*n* including three components: temporal balance based on mass conservation, capacity limits, and restoration after usage.

$$\begin{cases} \mathrm{LP}_{mn,t} = \mathrm{LP}_{mn,t-1} + \left(G^{\mathrm{in}}_{mn,t} - G^{\mathrm{ex}}_{mn,t}\right)\Delta t \\ \mathrm{LP}_{mn,t} \le \mathrm{LP}^{\max}_{mn} \\ \mathrm{LP}_{mn,t_N} = \mathrm{LP}_{mn,t_0} \end{cases}, \forall m,n \in J, \forall t \in T \tag{24}$$

where $\mathrm{LP}^{\max}_{mn}$ is the linepack capacity limit in pipeline *m*-*n*.

3.2.3 DHS constrains

In the DHS, the transportation of heat is subject to the nodal heat balance, which is expressed as [31]:

$$\sum_{k=1}^{K^{\mathrm{CHP}}}\left(H^{\mathrm{CHP}}_{k,t}\right) + \sum_{k=1}^{K^{\mathrm{GB}}}\left(H^{\mathrm{GB}}_{k,t}\right) + \sum_{k=1}^{K^{\mathrm{EB}}}\left(H^{\mathrm{EB}}_{k,t}\right) + \sum_{k=1}^{K^{\mathrm{HS}}}\left(H^{\mathrm{d}}_{k,t} - H^{\mathrm{c}}_{k,t}\right) - H^{\mathrm{l}}_{t} = \sum_{m=1}^{\Lambda^{\mathrm{n}}} H_{mn,t} \qquad \forall n \in K, \forall t \in T \tag{25}$$

where *K* sets the nodes of the DHS. The heat network follows the principle that the heat flows from nodes with higher temperature to lower temperature [15]. In the isobaric heating pipeline *m*-*n*, at time *t*, the thermal power flow is determined by the mass flow rate ($m_{mn,t}$) and the difference between the inlet temperature ($T^{\mathrm{in}}_{mn,t}$) and outlet temperature ($T^{\mathrm{out}}_{mn,t}$) of heating pipeline *m*-*n*.

$$H_{mn,t} = c \cdot m_{mn,t} \cdot \left(T^{\mathrm{in}}_{mn,t} - T^{\mathrm{out}}_{mn,t}\right) \qquad \forall m,n \in K, \forall t \in T \tag{26}$$

$$\sum_{m=1}^{\Lambda^{\mathrm{n}}} m_{mn,t} = 0 \qquad \forall n \in K, \forall t \in T \tag{27}$$

$$\frac{T^{\mathrm{out}}_{mn,t} - T^{\mathrm{a}}_{t}}{T^{\mathrm{in}}_{mn,t} - T^{\mathrm{a}}_{t}} = \exp\left(\frac{k_{mn}\pi d_{mn} l_{mn}}{c m_{mn,t}}\right) \qquad \forall m,n \in K, \forall t \in T \tag{28}$$

where *c*, k_{mn}, d_{mn} and l_{mn} represent the parameters of heating pipeline *m*-*n* including the specific heat capacity of water, the heat transfer coefficient, the diameter and the length, respectively. T^{a}_{t} is the ambient temperature at time *t*. Eq. (27) defines the conservation of nodal mass flow. Eq. (28) describes the temperature drop along the heating pipeline and reflects the heat loss in the DHS. Obviously, Eqs. (26) - (28) are nonlinear, causing a nonlinear optimization problem of the DHS. It is assumed that the DHS adopts the control strategy of

constant flow and variable temperature (CFVT) in which $m_{mn,t}$ is constant. Thus, the corresponding constraints become linear.

The limits of the heat transmission capacity can be expressed as:

$$\left|H_{mn,t}\right| \le H_{mn}^{\max} \qquad \forall m,n \in J, \forall t \in T \tag{29}$$

where $H_{mn}^{\max}$ is the maximum thermal power flow allowed by the heating pipeline *m*-*n*. The heat output limits of producers in the DHS are expressed as:

$$H_k^{\min} \le H_{k,t} \le H_k^{\max} \quad \forall k \in K^{\mathrm{CHP}} \cup K^{\mathrm{GB}} \cup K^{\mathrm{EB}}, \forall t \in T \tag{30}$$

where $H_k^{\min}$/ $H_k^{\max}$ is the minimum/maximum heat output of the heat producer *k*.

3.2.4 Energy conversion facilities

In this GHE-IES, multiple energy conversion facilities including CHP units, GBs, EBs and P2G units are introduced to achieve the energy supply across different energy subsystems. The relationship between the energy production and consumption of them can be respectively expressed as:

$$\begin{cases} P_{i,t}^{\mathrm{CHP}} = \eta_k^{\mathrm{CHP}} G_{j,t}^{\mathrm{CHP}} \\ P_{i,t}^{\mathrm{CHP}} = \eta_k^{\mathrm{P2H}} H_{k,t}^{\mathrm{CHP}} \end{cases} \quad \forall i \in I^{\mathrm{CHP}}, \forall j \in J^{\mathrm{CHP}}, \forall k \in K^{\mathrm{CHP}}, \forall t \in T \tag{31}$$

$$\eta_k^{\mathrm{P2H}} = \frac{\eta_k^{\mathrm{CHP}}}{\eta_k^{\mathrm{HE}} \cdot \left(1 - \eta_k^{\mathrm{CHP}} - \eta_k^{\mathrm{L}}\right)} \quad \forall k \in K^{\mathrm{CHP}} \tag{32}$$

$$H_{k,t}^{\mathrm{GB}} = \eta_k^{\mathrm{GB}} G_{j,t}^{\mathrm{GB}} \qquad \forall k \in K^{\mathrm{GB}}, \forall j \in J^{\mathrm{GB}}, \forall t \in T \tag{33}$$

$$H_{k,t}^{\mathrm{EB}} = \eta_k^{\mathrm{EB}} P_{i,t}^{\mathrm{EB}} \qquad \forall k \in K^{\mathrm{EB}}, \forall i \in I^{\mathrm{EB}}, \forall t \in T \tag{34}$$

$$G_{j,t}^{\mathrm{P2G}} = \eta_j^{\mathrm{P2G}} P_{i,t}^{\mathrm{P2G}} \qquad \forall j \in J^{\mathrm{P2G}}, \forall i \in I^{\mathrm{P2G}}, \forall t \in T \tag{35}$$

where η_k^{CHP}, η_k^{GB}, η_k^{EB} and η_j^{P2G} represent the conversion efficiencies of the CHP unit, the GB, the EB and the P2G unit, respectively. η_k^{P2H} is the power-to-heat ratio, which is determined by operational parameters of the CHP unit including the conversion efficiency from gas to power, the heat exchange coefficient (η_k^{HE}) and the heat loss coefficient (η_k^{L}). Since only the back-pressure CHP units are considered in this paper, the power-to-

heat ratio of any CHP unit is constant.

3.3 Solution methodology

As mentioned above, the equilibrium problem including optimization problems of the three energy subsystems is summarized as follows.

$$
\begin{aligned}
&\text{Find}\left(\boldsymbol{x}^{\text{EPS}}, \boldsymbol{x}^{\text{NGS}}, \boldsymbol{x}^{\text{DHS}}, \boldsymbol{p}\right) \text{satisfying, } \boldsymbol{p}=\left[p_t^{\text{e}}, p_t^{\text{g}}\right] \\
&\left(\boldsymbol{p}, \boldsymbol{x}^{\text{EPS}}\right) \in \arg\min f^{\text{e}}\left(\boldsymbol{x}^{\text{EPS}}, \boldsymbol{x}^{\text{EPS'}}, \boldsymbol{p}\right) \\
&\text{s.t.} \quad \begin{aligned} &h_i^{\text{e}}\left(\boldsymbol{x}^{\text{EPS}}, \boldsymbol{x}^{\text{EPS'}}\right)=0 \qquad i=1,2,3... \\ &g_i^{\text{e}}\left(\boldsymbol{x}^{\text{EPS}}, \boldsymbol{x}^{\text{EPS'}}\right) \le 0 \end{aligned}, \quad \boldsymbol{x}^{\text{EPS'}}=\left[P_{i,t}^{\text{EB}}, P_{i,t}^{\text{P2G}}\right] \\
&\left(\boldsymbol{p}, \boldsymbol{x}^{\text{NGS}}\right) \in \arg\min f^{\text{g}}\left(\boldsymbol{x}^{\text{NGS}}, \boldsymbol{x}^{\text{NGS'}}, \boldsymbol{p}\right) \\
&\text{s.t.} \quad \begin{aligned} &h_j^{\text{g}}\left(\boldsymbol{x}^{\text{NGS}}, \boldsymbol{x}^{\text{NGS'}}\right)=0 \qquad j=1,2,3... \\ &g_j^{\text{g}}\left(\boldsymbol{x}^{\text{NGS}}, \boldsymbol{x}^{\text{NGS'}}\right) \le 0 \end{aligned}, \quad \boldsymbol{x}^{\text{NGS'}}=\left[G_{j,t}^{\text{CHP}}, G_{j,t}^{\text{GB}}\right] \\
&\left(\boldsymbol{p}, \boldsymbol{x}^{\text{DHS}}\right) \in \arg\min f^{\text{h}}\left(\boldsymbol{x}^{\text{DHS}}, \boldsymbol{p}\right) \\
&\text{s.t.} \quad \begin{aligned} &h_k^{\text{h}}\left(\boldsymbol{x}^{\text{DHS}}\right)=0 \\ &g_k^{\text{h}}\left(\boldsymbol{x}^{\text{DHS}}\right) \le 0 \end{aligned} \qquad k=1,2,3...
\end{aligned}
\tag{36}
$$

where $\boldsymbol{x}^{\text{EPS'}}$ and $\boldsymbol{x}^{\text{NGS'}}$ represent variables that appear in their own subsystem but are controlled by other subsystems. They are subject to the linking constraints (31)-(35) of energy conversion devices. In the proposed equilibrium model, each subsystem agent controls its optimization problem. The corresponding variables and constraints are also controlled by or belong to exactly one subsystem agent. Variables that are controlled by one subsystem agent but appear in the equations of the other agents, the other agents consider them as fixed or exogenous variables. For a linear and convex optimization problem, KKT conditions are both necessary and sufficient. However, there is a non-convex Eq. (21) in the constraint of the NGS optimization. If the variation of the gas content in the pipeline is restricted within a narrow limit, Eq. (21) can be rewritten as a convex equation as shown in [9]. Hence, Lagrangian multiplier method is introduced to replace the original optimization problem to the new functions with KKT conditions as follows.

$$
\begin{aligned}
&L^{\mathrm{e}} = f^{\mathrm{e}}(\boldsymbol{x}^{\mathrm{EPS}}, \boldsymbol{x}^{\mathrm{EPS'}}, \boldsymbol{p}) - \sum_{i=1,2,3...} \boldsymbol{\lambda}_i^{\mathrm{e}} h_i^{\mathrm{e}}\left(\boldsymbol{x}^{\mathrm{EPS}}, \boldsymbol{x}^{\mathrm{EPS'}}\right) - \sum_{i=1,2,3...} \mu_i^{\mathrm{e}} g_i^{\mathrm{e}}\left(\boldsymbol{x}^{\mathrm{EPS}}, \boldsymbol{x}^{\mathrm{EPS'}}\right) = 0 \\
&L^{\mathrm{g}} = f^{\mathrm{g}}(\boldsymbol{x}^{\mathrm{NGS}}, \boldsymbol{x}^{\mathrm{NGS'}}, \boldsymbol{p}) - \sum_{j=1,2,3...} \boldsymbol{\lambda}_j^{\mathrm{g}} h_j^{\mathrm{g}}\left(\boldsymbol{x}^{\mathrm{NGS}}, \boldsymbol{x}^{\mathrm{NGS'}}\right) - \sum_{j=1,2,3...} \mu_j^{\mathrm{g}} g_j^{\mathrm{g}}\left(\boldsymbol{x}^{\mathrm{NGS}}, \boldsymbol{x}^{\mathrm{NGS'}}\right) = 0 \\
&L^{\mathrm{h}} = f^{\mathrm{h}}(\boldsymbol{x}^{\mathrm{DHS}}, \boldsymbol{p}) - \sum_{k=1,2,3...} \boldsymbol{\lambda}_k^{\mathrm{h}} h_k^{\mathrm{h}}\left(\boldsymbol{x}^{\mathrm{DHS}}\right) - \sum_{k=1,2,3...} \mu_k^{\mathrm{h}} g_k^{\mathrm{h}}\left(\boldsymbol{x}^{\mathrm{DHS}}\right) = 0 \\
&\text{K.K.T.} \quad \begin{cases}
\dfrac{\partial L^{\mathrm{e}}}{\partial \boldsymbol{x}^{\mathrm{EPS}}} = 0, \dfrac{\partial L^{\mathrm{g}}}{\partial \boldsymbol{x}^{\mathrm{NGS}}} = 0, \dfrac{\partial L^{\mathrm{h}}}{\partial \boldsymbol{x}^{\mathrm{DHS}}} = 0 \\
\mu_i^{\mathrm{e}} g_i^{\mathrm{e}}\left(\boldsymbol{x}^{\mathrm{EPS}}, \boldsymbol{x}^{\mathrm{EPS'}}\right) = 0, \mu_j^{\mathrm{g}} g_j^{\mathrm{g}}\left(\boldsymbol{x}^{\mathrm{NGS}}, \boldsymbol{x}^{\mathrm{NGS'}}\right) = 0, \mu_k^{\mathrm{h}} g_k^{\mathrm{h}}\left(\boldsymbol{x}^{\mathrm{DHS}}\right) = 0 \\
\boldsymbol{\lambda}_i^{\mathrm{e}}, \mu_i^{\mathrm{e}}, \boldsymbol{\lambda}_j^{\mathrm{g}}, \mu_j^{\mathrm{g}}, \boldsymbol{\lambda}_k^{\mathrm{h}}, \mu_k^{\mathrm{h}} \geq 0 \\
h_i^{\mathrm{e}}\left(\boldsymbol{x}^{\mathrm{EPS}}, \boldsymbol{x}^{\mathrm{EPS'}}\right) = 0, h_j^{\mathrm{g}}\left(\boldsymbol{x}^{\mathrm{NGS}}, \boldsymbol{x}^{\mathrm{NGS'}}\right) = 0, h_k^{\mathrm{h}}\left(\boldsymbol{x}^{\mathrm{DHS}}\right) = 0
\end{cases}
\end{aligned}
\tag{37}
$$

As show in Eq. (37), besides the original variables, the new sets of variables $\boldsymbol{\lambda}$ and $\boldsymbol{\mu}$ called 'Lagrange multipliers' are introduced. It should be noted that for the Nash equilibrium problem, all subsystem operators are on the same level, each assuming the decisions or strategies of the other agents are known and fixed. Therefore, the equilibrium problem of the proposed GHE-IES can be solved by jointly KKT conditions using PATH under GAMS.

4. Case studies

In this section, the combination of a 4-node NGS, a 4-bus EPS and an 8-node DHS is built as the test system, as shown in Fig. 3. The EPS has two generator nodes, two load nodes and four circuit branches. G2 and G3 are the wind turbine and the CFP unit, respectively. One EB and one P2G unit are installed at Bus 2. The NGS includes one source node, one load node and three pipe branches. One gas storage is installed at gas node (GN) 4 to facilitate the storage of the P2G unit production. G1 is the CHP unit, corresponding to Bus 1 in the power network and heat node (HN) 7 in the heat network. One GB is installed at GN 2, corresponding to HN 3 in the heat network. The DHS includes four nodes of the supply pipeline and four nodes of the return pipeline. Besides the facilities for heat supply mentioned above, one heat storage is installed at HN 1 to facilitate the heat storage of the CHP unit production. Tab. 1 and Tab. 2 show the related parameters of the test system.

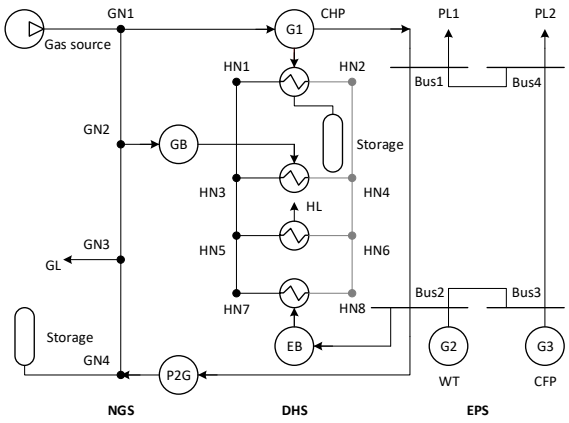

Fig. 3. Topology diagram of the test IES.

Table 1 Values of the marginal cost/utility parameters

Component	Parameter	Value (in €/MWh)
CFP	c_i^{CFP}	24
Gas source	c_j^{SN}	17.407
Gas storage	$c_j^{\mathrm{c}}/c_j^{\mathrm{d}}$	2/12
Heat storage	$c_k^{\mathrm{c}}/c_k^{\mathrm{d}}$	2/10
Power consumers	u^{PL}	30
Gas consumers	u^{GL}	25
Heat consumers	u^{HL}	20

Table 2 Values of the marginal cost/utility parameters

Energy Component	Parameter	Value	Unit
CHP	$P_i^{\mathrm{CHP,min}}/P_i^{\mathrm{CHP,max}}$	15/75	MW
	$P_i^{\mathrm{CHP,R}}$	30	MW
	η_k^{CHP}	80	%
	η_k^{P2H}	5:4	-
CFP	$P_i^{\mathrm{CFP,min}}/P_i^{\mathrm{CFP,max}}$	50/130	MW
	$P_i^{\mathrm{CFP,R}}$	25	MW
	η_k^{CFP}	50	%
P2G	$G_j^{\mathrm{P2G,min}}/G_j^{\mathrm{P2G,max}}$	0/16	MW
	η_j^{P2G}	40	%
GB	$H_k^{\mathrm{GB,min}}/H_k^{\mathrm{GB,max}}$	9.6/48	MW
	η_k^{GB}	90	%
EB	$H_k^{\mathrm{EB,min}}/H_k^{\mathrm{EB,max}}$	0/60	MW
	η_k^{EB}	100	%

Gas storage	$G_j^{c,max}/G_j^{d,max}$	5/5	MW
	$SOC_j^{GS,max}$	30	MWh
Heat storage	$H_k^{c,max}/H_k^{d,max}$	5/5	MW
	$SOC_k^{HS,max}$	20	MWh

The historical data obtained from Danish power, gas and heat systems are used in this study [32, 33]. The data of a typical day includes hourly gas, power and heat loads and hourly wind power production as shown in Fig. 4. To analyze the effect of different levels of wind power on the coordination of FRs and the market outcomes, two scenarios of low-wind within the output 7.2-63.4 MW and high-wind within the output 164-230 MW are chosen to simulate the test system as shown in Fig. 4 (b). It should be mentioned that the data have been scaled to fit this test study.

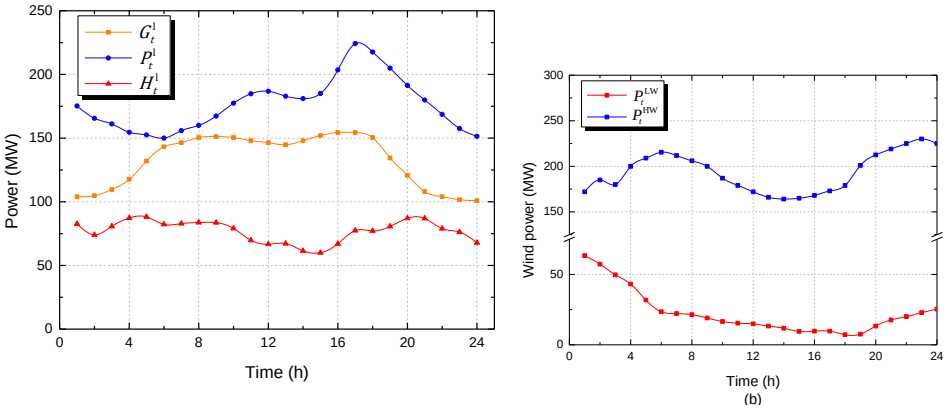

Fig. 4. Profiles of test data: (a) hourly gas, power and heat loads; (b) hourly low and high wind power profile.

For the daily operation of the test system in a 24-hour period, the equilibrium problem includes 1200 variables, 1368 inequality constraints, and 1128 equality constraints. Since this problem is a linear complementarity problem (NCP), it is solved using PATH solver under GAMS. The total computational time for each simulation is less than 15 seconds using a personal laptop with an Intel (R) Core (TM) i5 CPU clocking at 1.8 GHz and 8 GB of RAM.

4.1 Optimal operation and market interactions

In this section, LPF is set to 0.2, the integration and coordination of FRs are achieved by dispatching the GHE-IES. As one of the most important market outcomes, the price variation can reflect the energy exchange between different energy subsystems. Thus, to better observe the effect of different levels of wind power on the coordination operation and the market outcomes, the optimal operation strategy in a typical day under a low-wind scenario and a high wind scenario are shown in Fig. 5 and Fig. 6.

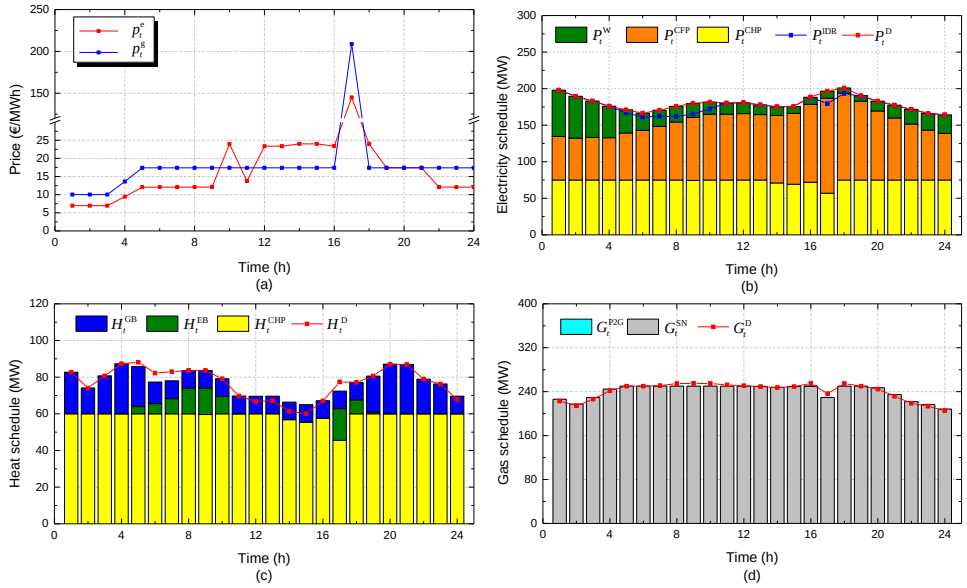

Fig. 5. Optimal operation strategy under the low-wind scenario: (a) daily energy price variation; (b) EPS scheduling; (c) DHS scheduling; (d) NGS scheduling.

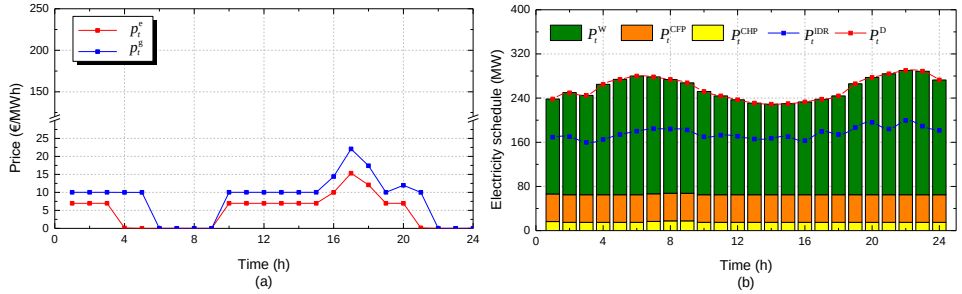

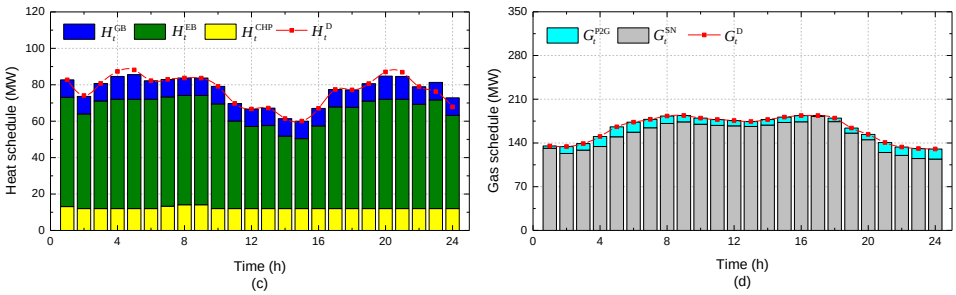

Fig. 6. Optimal operation strategy under the high-wind scenario: (a) daily energy price variation; (b) EPS scheduling; (c) DHS scheduling; (d) NGS scheduling.

For the low-wind scenario, the scheduling horizon can be divided into four periods based on the energy price variation in Fig. 5 (a). During the periods 1h-3h, there are enough wind power and a low gas load in the GHE-IES. Since the electricity and gas are cheap, the gas storage strives to store gas as shown in Fig. 7 (a). During the period 3h-16h, the wind power production begins to decrease rapidly, while the loads of electricity and gas are gradually increasing (Fig. 4). The electricity price and the gas price are respectively increasing to the marginal cost of the CFP unit (24 €/MWh) and the gas source (17.407 €/MWh), which causes the storage devices to start participating in energy supply (Fig. 7 (a)). Since the CHP unit has better economic performance, the DHS operator prefers to use it to supply heat and power as shown in Fig 5 (b) and (c). However, in the period 17h, there is a visible production curtailment of the CHP unit. The reason for this change is that the gas is unusually expensive at this time. More specifically, the energy shortage caused by the valley of wind power and the peak loads (Fig. 4), leads to the price peak of electricity (144.916 €/MWh) and gas (208.679 €/MWh). Since the peak price of gas is much higher than the peak price of electricity, the EPS operator and the DHS operator prefer to increase production of the EB and the CFP unit. During the period 17h-24h, as the wind power increases and the loads of gas and electricity decrease, the energy prices decrease and the gas storage stores gas with a satisfying price again (Fig. 7 (a)). It should be noted that the gas demand is almost entirely supplied by the gas source in the low-wind scenario (Fig. 5 (d)).

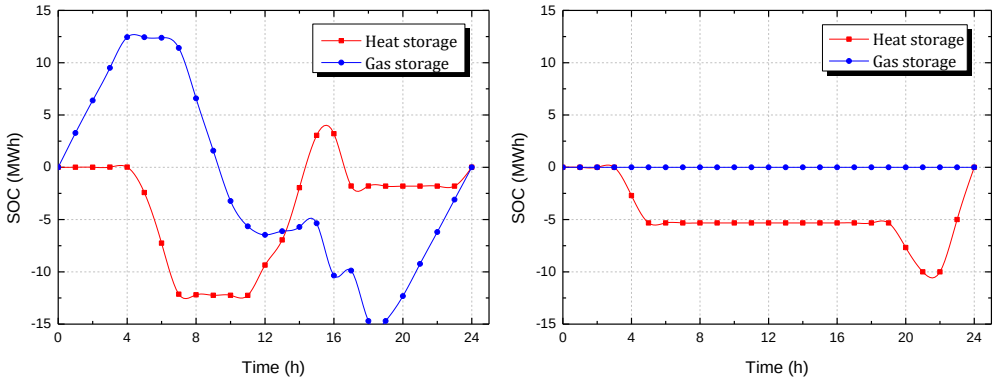

Fig. 7. SOC of the energy storages under two scenarios: (a) low-wind scenario; (b) high-wind scenario.

For the high-wind scenario, the scheduling horizon can be divided into three periods based on the energy price variation in Fig. 6 (a). During the periods 1h-3h and 10h-15h, a large amount of available wind power causes a significant reduction in the electricity price (6.963 €/MWh) and the gas price (10.026 €/MWh). On the one hand, the DHS operator prefers to use the EB to supply heat because of the cheap electricity (Fig. 6 (c)). On the other hand, the surplus wind power can be converted to gas by the P2G unit (Fig. 6 (d)), which leads to the utilization and the cost of the gas storage device (Fig. 7 (b)). During the periods 4h-9h and 21h-24h, with the peak of wind power generation, the prices of electricity and gas are reduced to zero, which can be regarded as the marginal cost of wind power. Due to the capacity limits of the EB and the P2G unit, there is still wind power curtailment in the GHE-IES. During the periods 16h-20h, the peak loads of all subsystems and low wind power generation cause the peak of the electricity price (15.332 €/MWh) and the peak of the gas price (22.078 €/MWh). It should be noted that in the high-wind scenario, a large number of wind power is effectively used with the coordination and integration of FRs, and the extreme prices of electricity and gas during peak-load periods are improved.

4.2 Positive impacts of FRs coordination

To further observe the positive impact of different FRs on the operation of the GHE-IES, the test system

is simulated in the six cases under the high-wind scenario. The case settings and simulation results are shown in Tab. 3. The results show that with the increase of coordinated FRs, the total social welfare of the GHE-IES increases, while the wind power curtailment decreases. Comparing the results of Case 1, 2, 3 and 6, the utilization of EBs, P2G units and DR management has a significant effect on reducing wind power curtailment. On the one hand, EBs and P2G units build new bridges of the power flow for the EPS, which leads to the electricity consumption no longer limited to its own system. Both the DHS and the NGS can provide additional flexibility and integrate more wind power. On the other hand, DR management flats the power load profile based on the market price. More specifically, this bi-directional feedback between DR management and the real-time electricity price helps relieve the mismatch between wind power generation and electricity loads.

Table 3 Total social welfare and wind power curtailment in different cases

Case	Setting	TSW (€)	WPC (MW)
1	CFP, GB, CHP, WF	89962	2444.4
2	CFP, GB, CHP, WF, P2G	96083	1523.1
3	CFP, GB, CHP, WF, EB	98041	752.9
4	CFP, GB, CHP, WF, EB, P2G	120480	217.7
5	CFP, GB, CHP, WF, EB, P2G, GS, HS	120530	205.0
6	CFP, GB, CHP, WF, EB, P2G, GS, HS, DR (LPF=0.2)	122270	23.92

TSW: Total social welfare; WPC: wind power curtailment

Considering different DR participation levels, Fig. 8 shows the simulation results of the used capacity of the heat storage, total social welfare and wind power curtailment under the high-wind scenario. Since the consumers that are willing to participate in DR management are limited in practice, this paper only analyzes the cases of LPF$\leqslant$0.35. Fig. 8 (a) demonstrates that with higher LPF, the used capacity of the heat storage reduces, which may cause a reduction in the investment of energy storage capacity. In addition, Fig. 8 (b) shows that with the higher DR participation level, the total social welfare increases and the wind power curtailment decreases in the GHE-IES. The above results indicate that DR management can avoid the power network congestions, reduce the requirement of storage capacity and improve wind power accommodation.

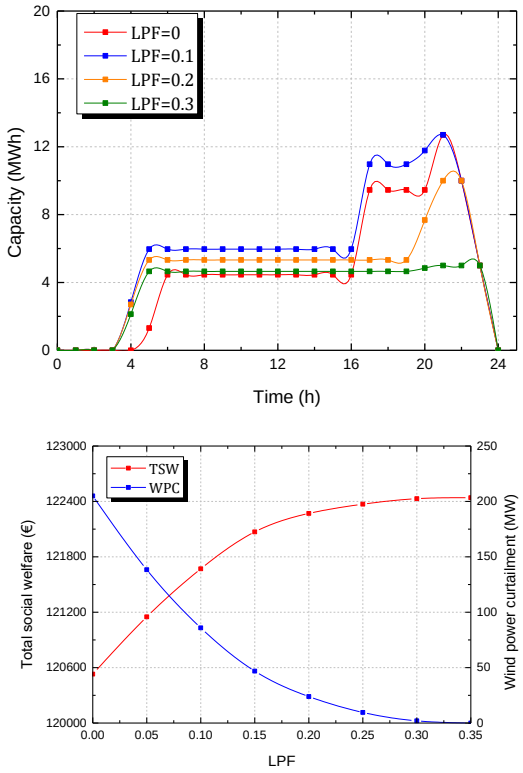

Fig. 8. The impact of different DR participation levels under the high-wind scenario: (a) used capacity of the heat storage; (b) total social welfare and wind power curtailment.

5. Conclusions

This paper investigates the optimal coordination of FRs of different energy systems under the short-term market. Based on the energy conversion technologies including CHP units, P2G units, GBs and EBs, a typical GHS-IES of the urban area in Denmark is firstly described in which consumers have multiple options for satisfying their demand. The FRs used include the flexible energy demand side, hourly DR management and multiple energy storages. Then, an equilibrium model is proposed to describe the gaming process of subsystem operators in the market, where each subsystem operator pursues its own benefit until an equilibrium is achieved. This paper focuses on the impact of coordination of FRs on the operation of the IES

and the market outcomes. The simulation results show that (1) the proposed model can make an optimal operation strategy according to the different levels of wind power, more specifically, in the high-wind scenario, wind power is effectively used through the coordination of FRs; (2) as the increase of coordinated FRs, the total social welfare and the wind power curtailment of the GHE-IES are significantly improved; (3) DR management realizes bi-directional feedback on the EPS consumption and affects electricity prices of the market, leading to the improvement of the abnormal peak price and the reduction of the requirement for the storage capacity.

Acknowledgements

The EUDP Project 'Sustainable Energy Market Integration (SEMI)' supports this work (EUDP17-I: 12554) In addition, the authors gratefully acknowledge the support of China Scholarship Council.

References

[1] Lund H, Østergaard PA, Connolly D, Mathiesen BV. Smart energy and smart energy systems. Energy 2017; 137: 556 – 565.

[2] The Danish commission on climate change policy. <https://ens.dk/en/our-responsibilities/energy-climate-politics/danish-climate-policies> [Accessed: 14. 06. 2012].

[3] Liu X, Mancarella P. Modelling, assessment and Sankey diagrams of integrated electricity-heat-gas networks in multi-vector district energy systems. Appl Energy 2016; 167: 336–352.

[4] Wang YL, Wang YJ, Huang Y, Li F, Zeng M, et al. Planning and operation method of the regional integrated energy system considering economy and environment. Energy 2019; 171: 731–750.

[5] Hansen K, Breyer C, Lund H. Status and perspectives on 100% renewable energy systems. Energy 2019; 175: 471-480.

[6] Bloess A, Schill WP, Zerrahn A. Power-to-heat for renewable energy integration: A review of technologies, modeling approaches, and flexibility potentials. Appl Energy 2018; 212: 1611–1626.

[7] Zhang Y, Campana PE, Yang Y, Stridh B, Lundblad A, Yan J. Energy flexibility from the consumer: Integrating local electricity and heat supplies in a building. Appl Energy 2018; 223: 430–442.

[8] Heydarian-Forushani E, Golshan MEH, Shafie-khah M, Siano P. Optimal operation of emerging flexible resources considering sub-hourly flexible ramp product. IEEE Trans Sustain Energy 2018; 9: 916–929.

[9] Fang J, Zeng Q, Ai X, Chen Z, When J. Dynamic optimal energy flow in the integrated natural gas and electrical power systems. IEEE Trans Sustain Energy 2018; 9: 188–198.

[10] Qadrdan M, Cheng M, Wu J, Jenkins N. Benefits of demand-side response in combined gas and electricity networks. Appl Energy 2017; 192: 360–369.

[11] Li Z, Wu W, Shahidehpour M, Wang J, Zhang B. Combined heat and power dispatch considering pipeline energy storage of district heating network. IEEE Trans Sustain Energy 2016; 7: 12–22.

[12] Troitzsch S, Sreepathi BK, Huynh TP, Moine A, Hanif S, et al. Optimal electric-distribution-grid planning considering the demand-side flexibility of thermal building systems for a test case in Singapore. Appl Energy 2020; 273: 114917.

[13] Wang Y, Ma YZ, Song F, Ma Y, Qi C, et al. Economic and efficient multi-objective operation optimization of integrated energy system considering electro-thermal demand response. Energy 2020; 205: 118022.

[14] Zhou H, Zheng JH, Li Z, Wu QH, Zhou XX. Multi-stage contingency-constrained co-planning for electricity-gas systems interconnected with gas-fired units and power-to-gas plants using iterative Benders decomposition. Energy 2019; 180: 689–701.

[15] Zeng Q, Zhang B, Fang J, Chen Z. A bi-level programming for multistage co-expansion planning of the integrated gas and electricity system. Appl Energy 2017; 200: 192–203.

[16] Samadi P, Mohsenian-Rad H, Schober R, Wong VWS. Advanced demand side management for the future smart grid using mechanism design. IEEE Trans Smart Grid 2012; 3: 1170–1180.

[17] Wang Y, Ai X, Tan Z, Yan L, Liu S. Interactive dispatch modes and bidding strategy of multiple virtual power plants based on demand response and game theory. IEEE Trans Smart Grid 2016; 7: 510–519.

[18] Chen S, Conejo AJ, Sioshansi R, Wei Z. Equilibria in electricity and natural gas markets with strategic offers and bids. IEEE Trans Power Syst 2020; 35: 1956–1966.

[19] Ruiz C, Conejo AJ, García-Bertrand R. Some analytical results pertaining to Cournot models for short-term electricity markets. Electr Power Syst Res 2008; 78: 1672–1678.

[20] Papaefthymiou G, Hasche B, Nabe C. Potential of heat pumps for demand side management and wind power integration in the German electricity market. IEEE Trans Sustain Energy 2012; 3: 636–642.

[21] Shao C, Ding Y, Wang J, Song Y. Modeling and integration of flexible demand in heat and electricity integrated energy system. IEEE Trans Sustain Energy 2017; 9: 361–370.

[22] Pozo D and Contreras J. Finding Multiple Nash Equilibria in Pool-Based Markets: A Stochastic EPEC Approach. IEEE Trans Power Syst 2011; 26:1744–1752.

[23] Schweppe FC, Caramanis MC, Tabors RD, Bohn RE. Spot pricing of electricity. Springer-Verlag US, 1988.

[24] Aalami HA, Parsa-Moghaddam, Yousefi GR. Demand response modeling considering Interruptible /Curtailable loads and capacity market programs. Appl Energy 2010; 87: 243–250.

[25] Conejo AJ, Morales JM, Baringo L. Real-time demand response model. IEEE Trans Smart Grid 2010; 1: 236–242.

[26] Xiao H, Pei W, Dong Z, Kong L. Bi-level planning for integrated energy systems incorporating demand response and energy storage under uncertain environments using novel metamodel. CSEE Journal of Power and Energy Syst 2018; 4: 155–167.

[27] Mohammadi S, Mohammadi A. Stochastic scenario-based model and investigating size of battery energy storage and thermal energy storage for micro-grid. Int J Electr Power Energy Syst 2014; 61: 531–546.

[28] Correa-Posada CM, Sánchez-Martín P. Integrated power and natural gas model for energy adequacy in short-term operation. IEEE Trans Power Syst 2015; 30: 3347–3355.

[29] Qiu J, Dong ZY, Zhao JH, Meng K, Zheng Y, Hill DJ. Low carbon oriented expansion planning of integrated gas and power systems. IEEE Trans Power Syst 2015; 30: 1035–46.

[30] Chaudry M, Jenkins N, Strbac G. Multi-time period combined gas and electricity network optimization. Electr Power Syst Res 2008; 78: 1265–79.

[31] Zeng Q, Fang J, Chen Z, Conejo AJ. A two-stage stochastic programming approach for operating multi-energy systems. 2017 IEEE Conference on Energy Internet and Energy System Integration (EI2), Beijing.

[32] Energinet.dk - Download of market data. <https://en.energinet.dk/> [Accessed: 01. 06. 2019].

[33] Danish Energy Agency - Technology Catalogs. <https://ens.dk/en/our-services/projections-and-models/technology-data > [Accessed: 23. 04. 2019].

Formatted: English (United States)